

isotherms at $t^* = 0.5$ and those at an earlier time ($t^* = 0.1$). In an attempt to exemplify the nature of the oscillations, the pointwise response of the velocity components at the origin is plotted in Fig. 1b. Here, evidence is solid that both horizontal and vertical velocities fluctuate in time in a somewhat irregular fashion without any indication to convince the existence of a steady-state solution.

Figures 2a–2d illustrate the influence of various parameters on the average heat and mass transfer rates as represented by the Nusselt and Sherwood numbers along the left wall. As noticed from Figs. 2a and 2b, an increase of the oblique angle results in an increase of heat and mass transfer rate, but the range of the buoyancy ratio within which oscillations occur does not appear to be affected while θ changes from $\pi/4$ to $\pi/3$. Unlike the oblique angle, the permeability ratio R is much more influential on the transport processes. Evidence from Figs. 2b and 2c confirms that it controls not only the transfer rates, but also the nature of thermosolutal convection. The latter may be seen through comparison of the history curves of the Nusselt and Sherwood numbers for $B = 0.5$, where the transport is modified from a stable regime to a stationary oscillatory regime. To assess the effects caused by the inclination angle γ , the Nusselt and Sherwood numbers were calculated for two configurations with $\gamma = \pi/3$ and $\pi/4$ and were plotted in Figs. 2c and 2d, respectively. Upon inspection of these figures, it is found that an enclosure with a larger inclination angle is more susceptible to oscillation. Also, for a fixed buoyancy ratio, the larger the inclination angle, the higher the heat and mass transfer rates.

IV. Concluding Remarks

The phenomenon of double diffusion in a trapezoidal enclosure filled with an anisotropic porous material having oblique principal axes has been investigated by means of a numerical method. The results have led to the following conclusions:

- 1) Flow oscillations only occur in a certain range of the buoyancy ratio that is dictated by the anisotropy of the medium as well as the inclination angle of the enclosure.
- 2) Heat and mass transfer is suppressed in trapezoidal enclosures with a small inclination angle.

Acknowledgments

This work was performed under the auspices of the U.S. Department of Energy, Contract DE-AC07-94ID13223, and is supported through the Idaho National Engineering Laboratory Long-Term Research Initiative in Computational Mechanics.

References

- ¹Nield, D. A., and Bejan, A., *Convection in Porous Media*, Springer-Verlag, New York, 1992.
- ²Kvernøld, O., and Tyvand, P. A., "Nonlinear Thermal Convection in Anisotropic Porous Media," *Journal of Fluid Mechanics*, Vol. 90, Pt. 4, 1979, pp. 609–624.
- ³Tyvand, P. A., "Thermohaline Instability in Anisotropic Porous Media," *Water Resources Research*, Vol. 16, No. 2, 1980, pp. 325–330.
- ⁴Nilsen, T., and Storesletten, L., "An Analytical Study on Natural Convection in Isotropic and Anisotropic Porous Channels," *Journal of Heat Transfer*, Vol. 112, May 1990, pp. 396–401.
- ⁵Kimura, S., and Masuda, Y., "Natural Convection in an Anisotropic Porous Medium Heated from the Side (Effects of Anisotropic Properties of Porous Matrix)," *Heat Transfer—Japanese Research*, Vol. 22, No. 2, 1993, pp. 139–153.
- ⁶Chang, W., and Lin, H., "Natural Convection in a Finite Wall Rectangular Cavity Filled with an Anisotropic Porous Medium," *International Journal of Heat and Mass Transfer*, Vol. 37, No. 2, 1994, pp. 303–312.
- ⁷Chang, W., and Hsiao, C., "Natural Convection in a Vertical Cylinder Filled with Anisotropic Porous Media," *International Journal of Heat and Mass Transfer*, Vol. 36, No. 13, 1993, pp. 3361–3367.
- ⁸Nguyen, H. D., Paik, S., and Douglass, R. W., "A Study of Double-Diffusive Convection in Layered Anisotropic Porous Media," *Numerical Heat Transfer, Part B*, Vol. 26, No. 4, 1994, pp. 489–505.

⁹Tyvand, P. A., and Storesletten, L., "Onset of Convection in an Anisotropic Porous Medium with Oblique Principal Axes," *Journal of Fluid Mechanics*, Vol. 226, May 1991, pp. 371–382.

¹⁰Zhang, X., Nguyen, T. H., and Kahawita, R., "Convective Flow and Heat Transfer in an Anisotropic Porous Layer with Principal Axes Non-Coincident with the Gravity Vector," *American Society of Mechanical Engineers, HTD-Vol. 264*, 1993, pp. 79–86.

¹¹Degan, G., Vasseur, P., and Bilgen, E., "Convective Heat Transfer in a Vertical Anisotropic Layer," *International Journal of Heat and Mass Transfer*, Vol. 38, No. 11, 1995, pp. 1975–1987.

¹²Aboubi, K., Robillard, L., and Bilgen, E., "Natural Convection in Horizontal Annulus Filled with an Anisotropic Porous Medium," *ASME/JSME Thermal Engineering Conference*, Vol. 3, 1995, pp. 415–422.

¹³Dong, Z. F., and Ebdian, M. A., "Investigation of Double-Diffusive Convection in a Trapezoidal Enclosure," *Journal of Heat Transfer*, Vol. 116, May 1994, pp. 492–495.

Hydromagnetic Free Convection Flow Over an Inclined Plate Caused by Solar Radiation

Ali J. Chamkha*

Kuwait University, Safat 13060, Kuwait

Introduction

THIS Note discusses steady, laminar, two-dimensional, free convection flow of water up an inclined flat plate in the presence of a uniform transverse magnetic field and solar radiation. Heating to the plate is supplied by the absorbing and electrically conducting working fluid (water), which receives incident rays of solar radiation. This flow situation has possible application in natural water bodies; crystal growth; solar-energy collectors with direct solar-energy collection and storage using absorbing fluids such as ammonia, carbon dioxide, and water; geothermal reservoirs, solar heating systems, packed-bed catalytic reactors, and cooling of nuclear reactors. The geothermal gases are electrically conducting and undergo the influence of the magnetic field. The same is found regarding the cooling of nuclear reactors.¹ Nonmagnetic natural convection from a heated plate has been considered by many investigators.^{2–4} The effects of magnetic field on free convection from a vertical flat plate and other geometries have also been studied.^{5–7} It is of interest in this Note to generalize the work of Fathalah and Elsayed⁴ by including a uniform transverse magnetic field and plate-tilting effects. The semi-infinite inclined flat plate is assumed to be nonreflecting, nonabsorbing, and ideally transparent. It is also assumed that the plate receives solar incident radiation flux that penetrates its surface and is absorbed by the absorbing fluid. By interaction with the absorbing fluid, both heat transfer from the fluid to the wedge and heat loss from the plate surface to the surroundings take place. The fluid is assumed Newtonian, absorbing, electrically conducting, and isotropic. The magnetic Reynold's number is assumed to be small so that the induced magnetic field can be neglected. Also, since there is no applied electric field, the effect of polarization and the Hall effect of magnetohydrodynamics are neglected.

Received Feb. 26, 1996; revision received Nov. 20, 1996; accepted for publication Nov. 26, 1996. Copyright © 1997 by the American Institute of Aeronautics and Astronautics, Inc. All rights reserved.

*Assistant Professor, Department of Mechanical and Industrial Engineering, P.O. Box 5969.

Mathematical Formulation

Consider steady hydromagnetic free convection boundary-layer flow of an electrically conducting and absorbing fluid over an inclined plate. The coordinate system is such that x measures the distance along the plate surface and y measures the distance normally outward. A transverse magnetic field of constant strength is applied normal to the flow direction. Both the surrounding and the absorbing fluid far away from the inclined plate surface are maintained at a constant temperature T_∞ . The governing equations for this problem can be written as follows⁸:

$$\frac{\partial u}{\partial x} + \frac{\partial v}{\partial y} = 0 \quad (1)$$

$$u \frac{\partial u}{\partial x} + v \frac{\partial u}{\partial y} = \nu \frac{\partial^2 u}{\partial y^2} + g\beta(T - T_\infty)\cos\phi - \frac{\sigma B_0^2}{\rho} u \quad (2)$$

$$u \frac{\partial T}{\partial x} + v \frac{\partial T}{\partial y} = \frac{k}{\rho c} \frac{\partial^2 T}{\partial y^2} + \frac{1}{\rho c} \frac{\partial q''_{\text{rad}}}{\partial y} \quad (3)$$

where u , v , and T are the fluid velocity components in the x and y direction, and the fluid temperature, respectively. ρ , ν , c , and k are the fluid density, kinematic viscosity, specific heat, and thermal conductivity, respectively. g , β , and ϕ are the gravitational acceleration, coefficient of volumetric thermal expansion, and the inclined plate or wedge half-angle, respectively. q''_{rad} is the applied absorption radiation heat transfer per unit area. σ and B_0 are the fluid electrical conductivity and magnetic induction, respectively. Note that viscous and magnetic dissipations are neglected and all properties are assumed constant except the fluid density in the buoyancy term. In addition, the normal buoyancy component as well as the motion pressure that would arise because of the inclination against the flow are both neglected. This is justified for small angles up to 60 deg, as reported by Gebhart et al.⁸

The appropriate boundary and matching conditions for this problem are

$$u(x, 0) = 0 \quad (4a)$$

$$v(x, 0) = 0 \quad (4b)$$

$$k \frac{\partial T}{\partial y}(x, 0) = U[T(x, 0) - T_\infty] \quad (4c)$$

$$u(x, \infty) = 0 \quad (4d)$$

$$T(x, \infty) = T_\infty \quad (4e)$$

$$T(0, y) = T_\infty \quad (4f)$$

$$u(0, y) = 0 \quad (4g)$$

where U is the heat transfer coefficient for the heat loss from the plate to the surroundings.

Cooper⁹ and Fathalah and Elsayed⁴ reported that absorption radiation on water can be represented by Beer's law of radiation, as follows:

$$q''_{\text{rad}} = q''[1 - \exp(-ay)] \quad (5)$$

where the constants q'' and a are the incident radiation flux and the fluid's absorption coefficient, respectively.

Following Fathalah and Elsayed,⁴ the governing equations are nondimensionalized by using

$$u = \frac{\partial \psi}{\partial y} \quad (6a)$$

$$v = -\frac{\partial \psi}{\partial x} \quad (6b)$$

$$\xi = \frac{G_x}{G_a^5} \quad (6c)$$

$$\eta = \frac{yG_x}{5x} \quad (6d)$$

$$G_x = 5 \left(\frac{g\beta q'' x^4}{5k\nu^2} \right)^{1/5} \quad (6e)$$

$$G_a = 5 \left(\frac{g\beta q''}{5k\nu^2 a^4} \right)^{1/5} \quad (6f)$$

$$\psi = \nu G_x F(\xi, \eta) \quad (6g)$$

$$T = T_\infty - \frac{5xq''}{kG_x} \theta(\xi, \eta) \quad (6h)$$

where G_x and G_a are the local Grashof numbers based on x and a , respectively.

The substitution of Eqs. (5) and (6) into Eqs. (1-3), and simplifying, yields the following:

$$F''' + 4FF'' - 3F'^2 - \theta \cos\phi + 4\xi(GF'' - F'G') - 25\xi^{1/2}M^2F' = 0 \quad (7)$$

$$\theta'' + Pr(4F\theta' - F'\theta) - 4\xi Pr(F'H - \theta'G) - 5\xi^{1/4} \exp(-5\xi^{1/4}\eta) = 0 \quad (8)$$

where $Pr = \rho\nu c/k$ and $M^2 = \sigma B_0^2/(a\rho\nu)$ (B_0 being a constant) are the fluid Prandtl number and the square of the Hartmann number, respectively. In Eqs. (7) and (8), a prime denotes ordinary differentiation with respect to η , and G and H are the first derivatives of F and θ with respect to ξ , respectively.

The corresponding transformed dimensionless boundary and matching conditions can be written as

$$F(\xi, 0) = 0 \quad (9a)$$

$$F'(\xi, 0) = 0 \quad (9b)$$

$$\theta'(\xi, 0) = 5\alpha\xi^{1/4}\theta(\xi, 0) \quad (9c)$$

$$F'(\xi, \infty) = 0 \quad (9d)$$

$$\theta(\xi, \infty) = 0 \quad (9e)$$

$$\theta(0, \eta) = 0 \quad (9f)$$

$$F(0, \eta) = 0 \quad (9g)$$

where $\alpha = U/(ka)$ is the dimensionless heat transfer loss coefficient.

Equations (7) and (8) are nonsimilar. However, the approximate local nonsimilarity method employed by Fathalah and Elsayed⁴ can be applied for this problem. Additional equations and boundary conditions governing G and H are obtained by differentiating Eqs. (7-9) with respect to ξ . The resulting equations and boundary conditions are not written herein for brevity. However, the resulting ordinary differential equations (ODEs) for this problem are approximate since higher-order ξ derivative terms are neglected as required by the local similarity method. The equations reported by Fathalah and Elsayed⁴ are recovered by formally setting M and ϕ equal to zero.

Of special interest in this work are the local boundary-friction coefficient and the Nusselt number. These physical parameters can be defined in dimensional form as

$$B_f^* = \frac{-\mu\partial^2\psi(x, 0)}{\partial y^2} \quad (10a)$$

$$Nu_a = \frac{h}{ka} \quad (10b)$$

$$h = \frac{q'' - U(T_w - T_\infty)}{T_{\max} - T_\infty} \quad (10c)$$

where μ is the fluid dynamic viscosity, T_w is the plate or wall temperature, T_{\max} is the maximum local temperature, and h is the local heat transfer coefficient. The justification for the use of two unknown temperatures, T_w and T_{\max} , in the definition of the Nusselt number is contrary to radiation-free natural convection problems over a vertical plate, the maximum temperature does not occur at the plate surface. Upon using Eqs. (6), it can be shown that

$$B_f = \frac{B_f^*}{\rho v^2 G_x a^2} = -\frac{F''(0)}{25\xi^{1/2}} \quad (11a)$$

$$Nu_a = -\left(\frac{1}{5\xi^{1/4}\theta_{\max}} + \alpha \frac{\theta_w}{\theta_{\max}}\right) \quad (11b)$$

Results and Discussion

The resulting governing equations for this investigation are coupled nonlinear ODEs that exhibit no analytical solution and, therefore, must be solved numerically. The standard, implicit, iterative, tridiagonal finite difference numerical method similar to that discussed by Blottner¹⁰ is employed herein. For more details of the numerical method the reader is advised to read the paper by Blottner.¹⁰

It should be mentioned, however, that variable step sizes in η are employed with the initial step size $\Delta\eta_1$ being equal to 10^{-3} and the growth factor is set to 1.03. These values are arrived at after many numerical experiments performed to

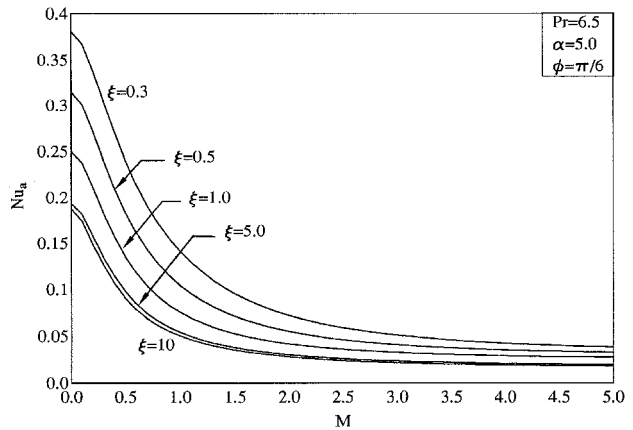


Fig. 3 Effects of ξ and M on Nusselt number.

assess grid independence. A convergence criterion based on the relative difference between two successive iterations that was set to 10^{-4} in the present work was utilized. Many numerical results were obtained throughout the course of this work. For brevity, only few graphical results for the Nusselt number will be reported.

Figures 1–3 illustrate the influence of Pr , α , the distance along the plate ξ , and the Hartmann number M , on Nu_a , respectively. It is observed from Fig. 1 that while Nu_a decreases as M increases, it increases as Pr increases. The increase in the Nu_a values as Pr increases is because of the reductions of the maximum temperature (occurring for higher values of Pr) since it is inversely proportional to it (see the definition of Nu_a given earlier). The small kinks appearing in this and the subsequent curves of Nu_a are a result of the choice of steps in the values of M employed to obtain the numerical results. Each point on these figures represents a separate computer run or calculation. Increases in the values of α have a tendency to reduce the fluid's temperature. This causes the slope of its profile at the wall to decrease, which has the direct effect of decreasing Nu_a , as is evident from Fig. 2. Figure 3 shows, as expected, that Nu_a decreases as ξ increases. This is consistent with the definition of Nu_a , which is inversely proportional to ξ . From other results not presented herein for brevity, it is also observed that Nu_a decreases as the angle ϕ increases.

For $M = 0$ and $\phi = 0$ (vertical flat plate) the results reported by Fathalah and Elsayed⁴ are recovered. This comparison serves as a check on the numerical procedure. Equations (7) and (8) were also solved subject to the appropriate boundary conditions by the same finite difference method discussed by Blottner.¹⁰ Few comparisons with the results obtained by the local similarity method showed that, for the parametric values employed, an error of about 1% resulted. Validation of the numerical results reported herein can be best done by direct comparisons with experimental data on the problem under consideration. However, such data appear to be lacking at present.

Conclusions

Hydromagnetic natural convection flow of an electrically conducting and absorbing fluid along an isothermal inclined plate in the presence of a uniform transverse magnetic field because of solar radiation is considered. The local similarity method is employed in this problem to allow comparisons with previously published work. The resulting approximate nonlinear ODEs are solved numerically by a standard implicit iterative finite difference method. Few representative numerical results for the Nusselt number are presented graphically and discussed. It was found that the Nusselt number based on the fluid's absorbing coefficient was increased as the Prandtl number increased and reductions were observed as a result of increasing the heat transfer loss coefficient, tangential distance, the Hartmann number, or the inclination angle. Comparison

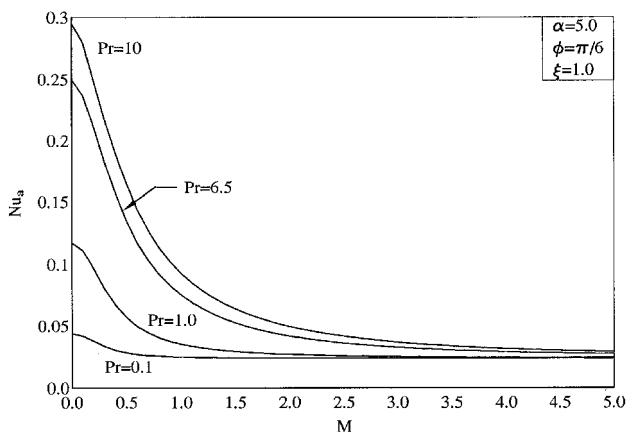


Fig. 1 Effects of Pr and M on Nusselt number.

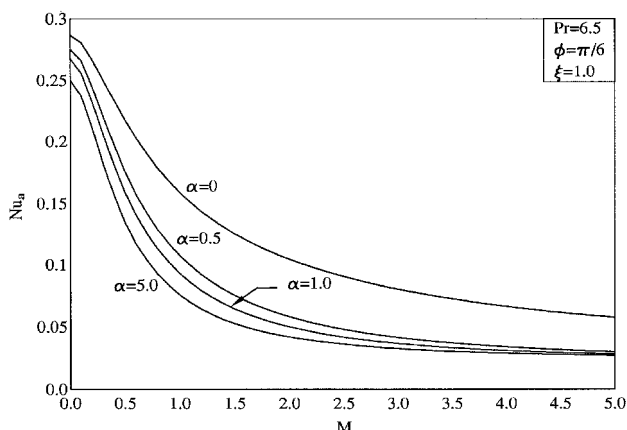


Fig. 2 Effects of α and M on Nusselt number.